Evaluation of PP and PS binning for a multicomponent seismic survey from west-central Alberta

Hussain Aldhaw and Donald C. Lawton

ABSTRACT

A multicomponent seismic survey undertaken recently in west-central Alberta is evaluated for PP and PS binning methods. A 50 km^2 subset of the real survey was selected for analysis and subsequent processing. A major step in seismic processing is binning and deciding on the optimum bin size, especially for PS data. One of the common methods is ACP (Asymptotic Common Point), because it requires only an average V_p/V_s ratio and the binning is independent of the depth of the target horizon.

The simulated design is used to test for the optimum ACP binning parameters. It was designed based on the acquisition parameters of the real survey, and on the analysis made on the synthetic data set. A synthetic seismogram was created by convolving well log reflectivity data (from V_p, V_s and density logs) from a nearby well with a wavelet that represents the data. The reflection amplitudes and transmission losses are calculated using the Zoeppritz equations. Maximum useable offset was chosen based on the actual survey geometry for the depth of interest. Then it was used for the simulated survey design to evaluate the fold and offset distribution for both PP and PS datasets of the field survey.

INTRODUCTION

A synthetic seismogram (or simply synthetic) is usually used to correlate seismic and well data and it is generated by using sonic and density logs to derive velocity and density data, respectively. Then, an acoustic impedance curve is generated. From this curve, we can compute reflection coefficients at each interface between contrasting velocities.

The other parameter needed is the wavelet:

*Synthetic seismogram = wavelet * reflection coefficient*, where (*) is convolution.

The wavelet is the link between synthetic traces and the geology (reflection coefficients) that is being interpreted. In this case, we have V_p, V_s and density logs with tops picked on them indicating our area of interest. Our target is Duvernay Formation which is around 3400 m deep. We create an offset synthetic seismogram that gives a strong interpretable response at that depth level considering the following parameters and phenomena: wavelet, maximum useable offset, NMO stretch and distortions, amplitude/phase issues as approaching critical angle and maximum offset to depth ratio. In this paper, we will determine the maximum usable offset from the synthetic data set. Then we will implement that, with the optimum bin size, to evaluate a simulated survey design for both P-P and P-S wave data.

BACKGROUND

For P wave data, the binning process is completed using conventional midpoint binning to create the grid for the survey. However, the P-S waves is assumed to be the conversion of P waves reflected from the interface to the receiver. Thus, the travel path of the P-S is asymmetric for flat reflectors which rules out the use of the standard common midpoint binning used for P waves data as a correct solution.

The raypaths of the converted waves are asymmetric and the reflection points in the subsurface are always closer to the receiver. Different techniques are required to stack such data where common conversion point (CCP) is considered instead of common mid-point (CMP) in the conventional surveys (Lawton, 1993). The CCP techniques could be asymptotic (Behle and Dohr, 1985; Fromm et al., 1985), single depth (Tessmer and Behle, 1988; Tessmer et al., 1990), depth-variant CCP mapping (Eaton et al, 1990; Stewart, 1991), and converted-wave DMO (Harrison, 1992). In this paper we will only consider the asymptotic approach (ACP).

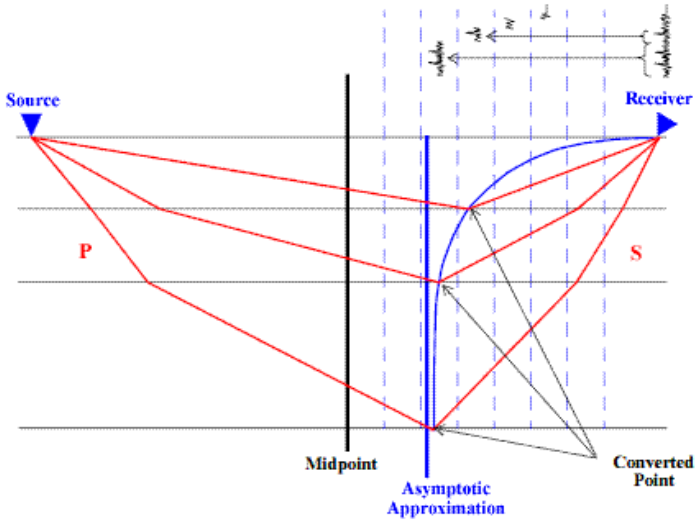

FIG. 1. Midpoint, Conversion points and asymptotic approximation

DATA

The real survey covers approximately 200 sq. km. A segment of that area was selected for processing. The simulated survey design is based on the segmented area. As for the well data, well logs are measured in a well that lies in the original big survey and nearby to the segmented area of the survey.

Well Data

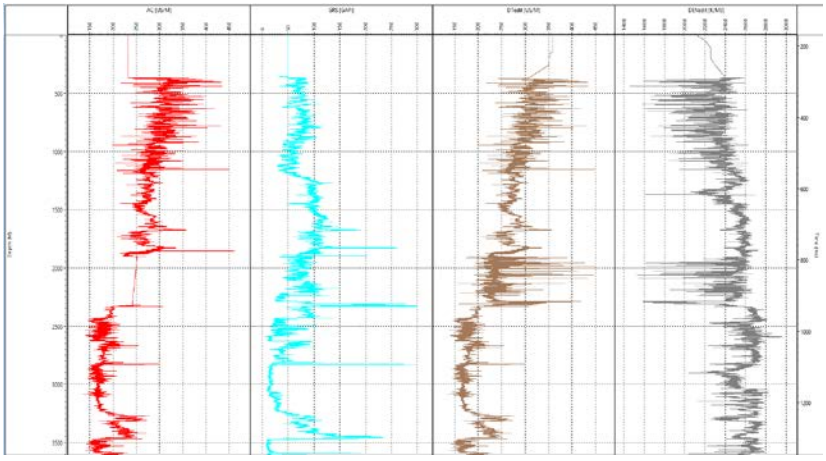

FIG. 2. Well logs from left to right: sonic interval transit time, gamma ray, delta transit time and bulk density

Acquisition Parameters

Table 1 Acquisition parameters for both real data and simulated surveys

Source Interval	60 m
Source Line Int	420 m
Receiver Interval	60 m
Receiver Line Int.	360 m

The software used to create the simulated survey design does not allow importing actual coordinates for shot and receivers. So, irregularities in the shots and receivers geometry in the real data cannot be honored, so is the number of shots and receivers but they are approximately the same. However, the shot and receiver interval, shot line and receiver line interval and survey type (orthogonal) is the same between both surveys. as shown in Figure 3.

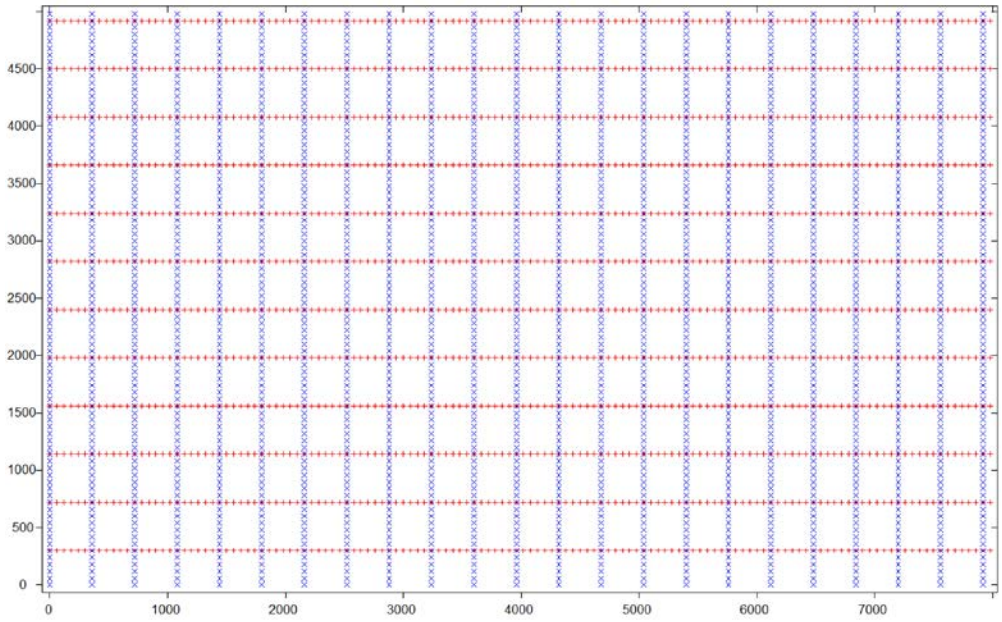

FIG. 3. Shot-receiver of the simulated survey design. Shot lines are E-W and receiver lines are N-S

SYNTHETIC DATA

To generate synthetic data set, CREWES SYNGRAM software was used. SYNGRAM creates primaries only synthetic seismograms for P-P and P-S reflections. The synthetic seismograms are trace gathers for a horizontally layered earth and show the variation of amplitude with offset as well as the stacked response. The reflection amplitudes, and optional transmission losses, are calculated from the Zoeppritz equations (no approximation) and are therefore appropriate for plane-wave incidence. Traveltimes and incidence angles are calculated by ray tracing.

SYNGRAM requires the input of both logs P-wave sonic (and S-wave sonic if available) and bulk density in addition to the wavelet. The layered earth model is provided to SYNGRAM in a consistent set of units. If an S-wave log is not available, then in order to create S-wave sonic log, the software assume a default value of V_p/V_s to be a user-defined value (typically 2). However, the V_p/V_s ratio used here is 2.01 according to Interval and surface-to-depth V_p/V_s ratios analysis made by (Weir et al. 2018) in the general area of interest, and summarized in Table 2.

Table 2 Interval and surface-to-depth V_p/V_s ratios. The row in blue is the measured P-S times, the column in green is the measured P-P times. V_p/V_s at the depth of interest SWH is 2.01. (Weir et al., 2018)

V_P/V_S	2WS	Doe Creek	Wab.	Ireton	Swan Hills	Gill	~Prec	PP time (ms)
Colo	**2.15**	1.99	2.15	2.09	2.05	2.07	2.18	971
2WS	1.991	**2.09**	1.88	1.86	1.981	2.02	2.156	1253
Wab.	2.148	1.88	**2.03**	1.80	1.78	1.94	2.06	1766
Ireton	2.088	1.88	1.80	**2.03**	1.814	2.09	2.06	1933
SWH	2.050	1.981	1.87	1.814	**2.01**	2.411	2.18	2000
Gill.	2.073	2.017	1.93	2.09	2.411	**2.02**	2.02	2068
~Prec.	2.179	2.02	2.06	2.06	2.18	2.02	**2.02**	2151
PS time (ms)	1484	1950	2674	2909	2994	3110	3298	V_P/V_S

For the wavelet, SYNGRAM allows to create different types of wavelets. The wavelets used here are bandpass wavelets for P-P and P-S data with parameters shown in Figure 4. Both wavelets were designed based on the processes P-P and P-S from the field survey. The wavelets designed are shown in Figure 5.

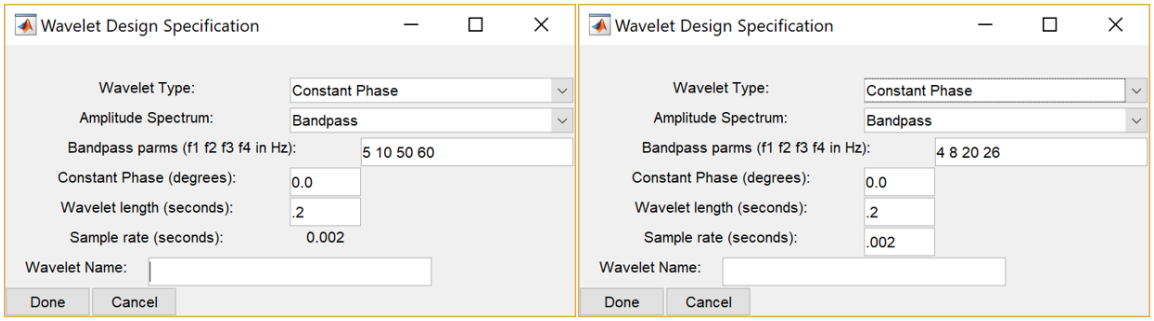

FIG. 4. Wavelet parameters for P-P (left) and P-S (right)

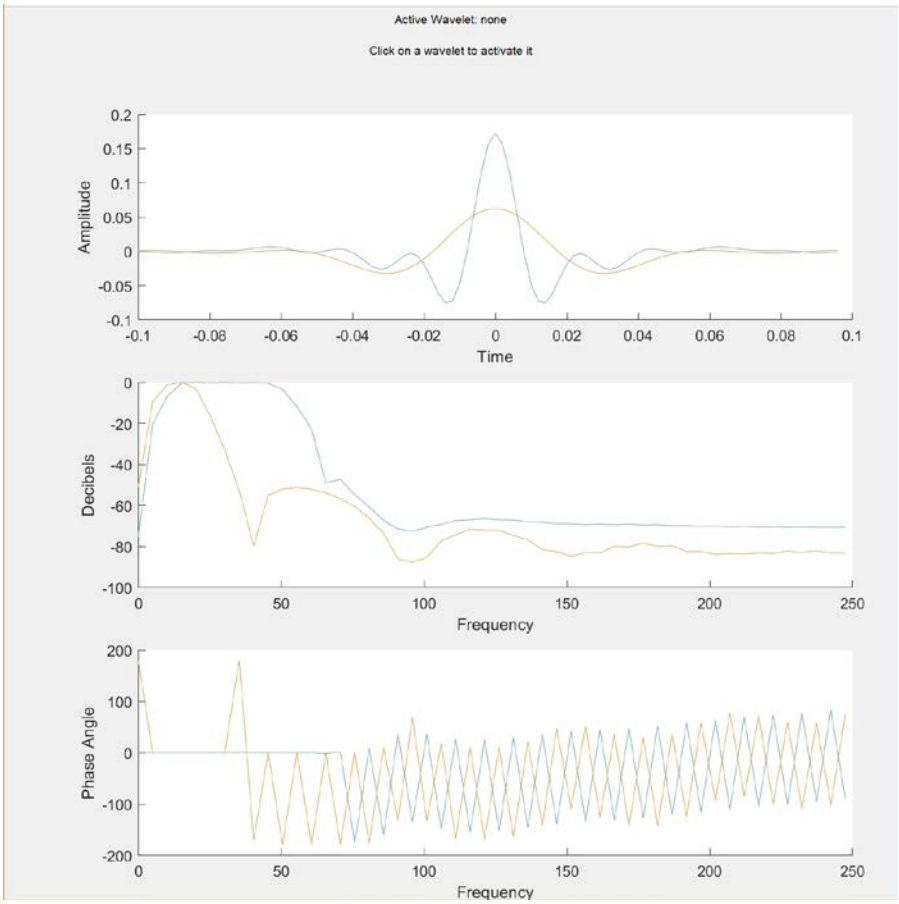

FIG. 5. P-P (green) and P-S (yellow) wavelets overlapped

Using both logs data and constructing the appropriate wavelets, SYNGRAM convolves the earth model given by the well logs with the wavelets to generate synthetic offset gathers and stacks for both P-P and P-S. The maximum offset from the real data survey is approximately 6200 m. To include all of these offsets, the maximum offset-depth ratio is set to be 2.

Initial P-P and P-S seismograms generated are shown in Figure 6. The interval of interest is between 3350 to 3450 m, which is the area between Devonian Woodbend and Duvernay formations. Both of the synthetic seismograms included overlays of the incident angles for each depth step. At source-receiver offsets beyond approximately 4000 m, there are significant distortions due to critical incident angles.

Synthetic data set analysis

Changing the maximum offset-depth ratio allows us to mute distorted traces at far offsets. So, the offset-depth ratio works as a mute function excluding uninterpretable traces. Ratios used in Figure 7 are 1.3 and 1.5 for P-P and P-S, respectively.

Analyzing both synthetic seismograms, a stretch and phase rotation are observed in some traces at certain offsets and depths. That will help us decide on the maximum useable offsets when we design our P-P and P-S surveys. Our target is at 3400 – 2430 m deep. Traces at that depth are distorted around 3000 m offset as shown in Figure 7.

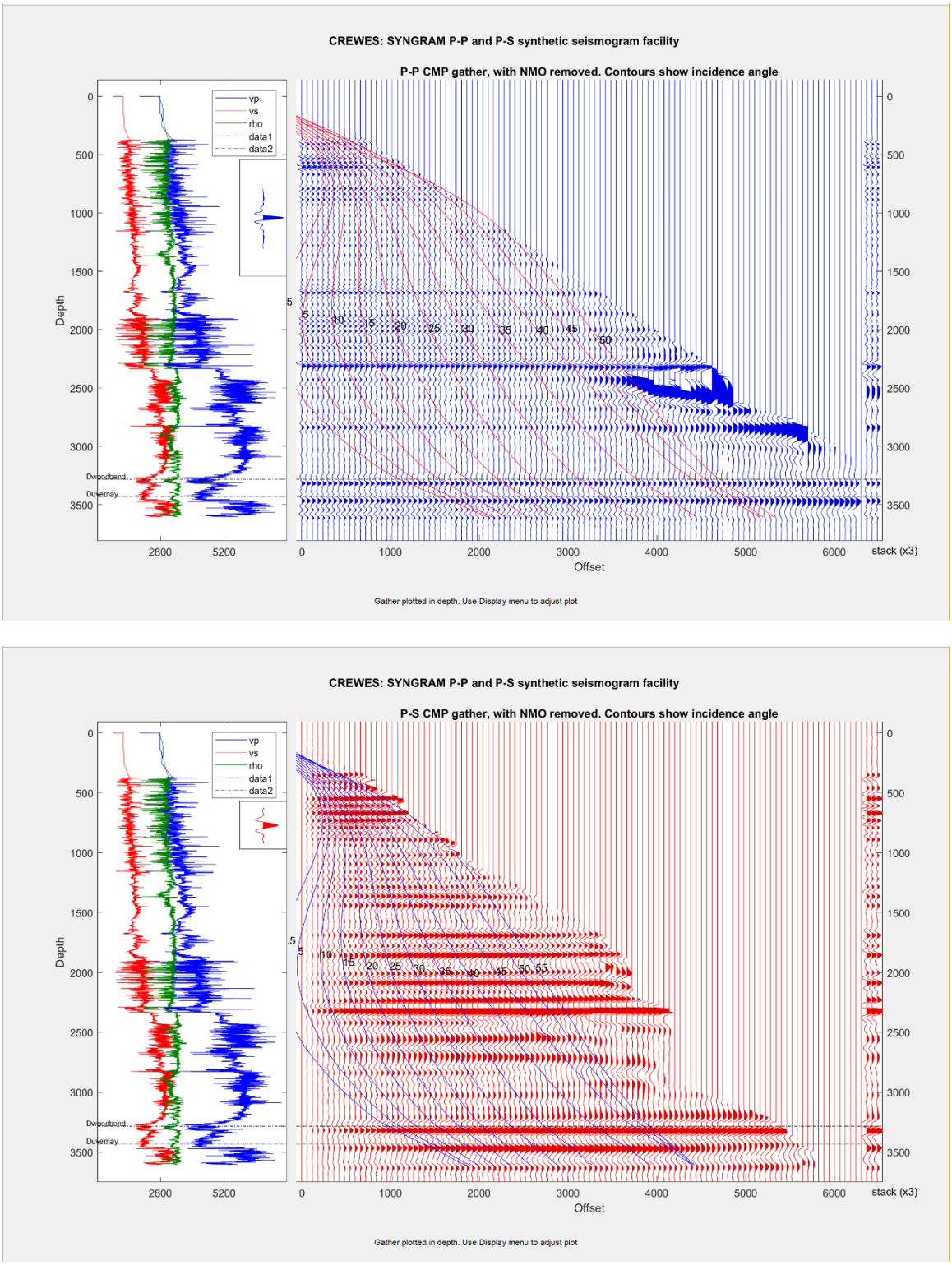

FIG. 6. Synthetic offset gathers for P-P (top) and P-S (bottom). V_s log was generated based on the relation $V_p/V_s = 2.01$. (amplitudes were scaled in both seismograms)

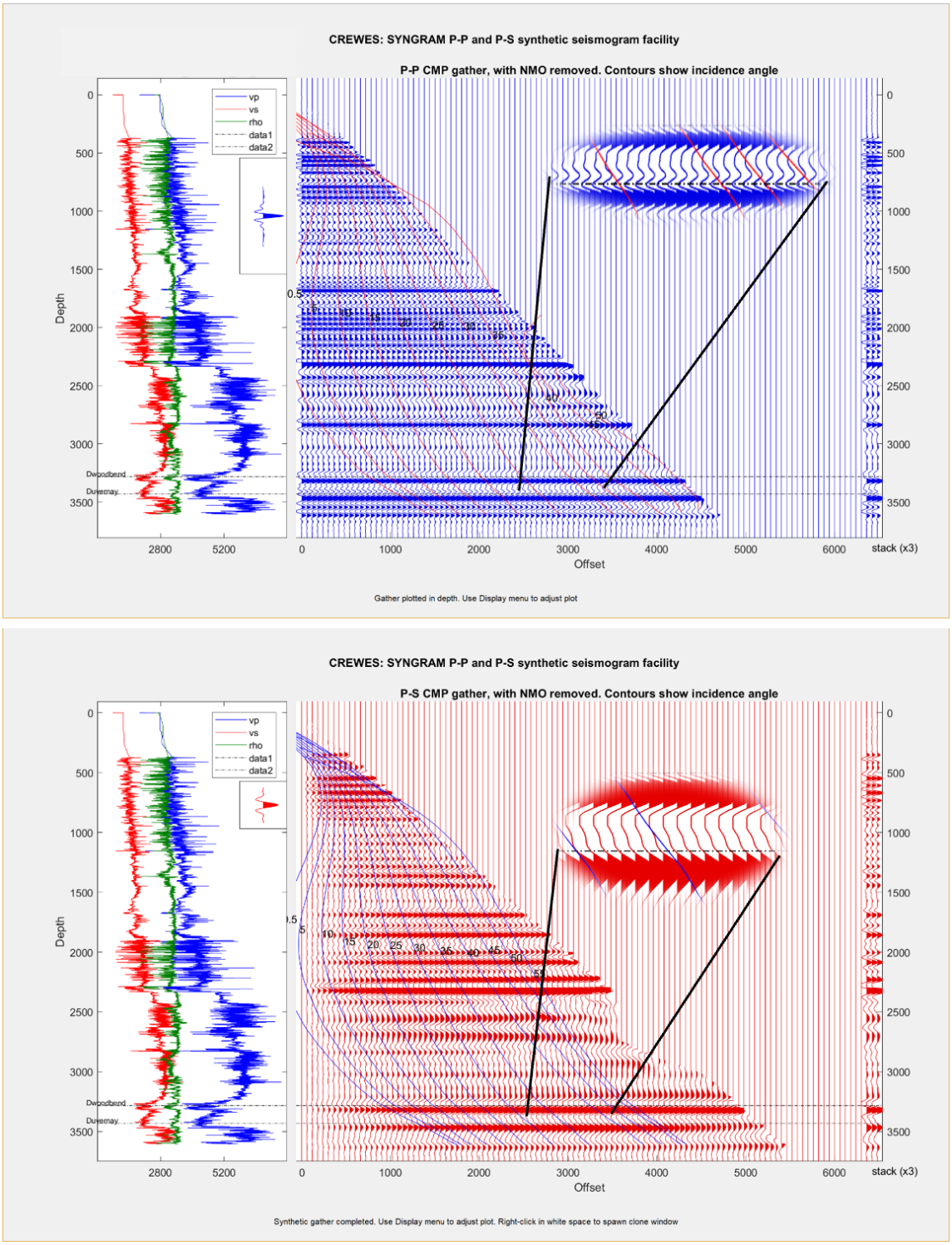

FIG. 7. Traces start to get distorted for P-P (top) and P-S (bottom) around offset 3000 m. So, the maximum useable offset will be used for P-P and P-S designs is 3000 m

When both stacks are compared using the maximum offset-depth ratio above, we see a good tie along the whole section as in Figure 8. That means that the bad distorted and polarity flipped traces were excluded from the data.

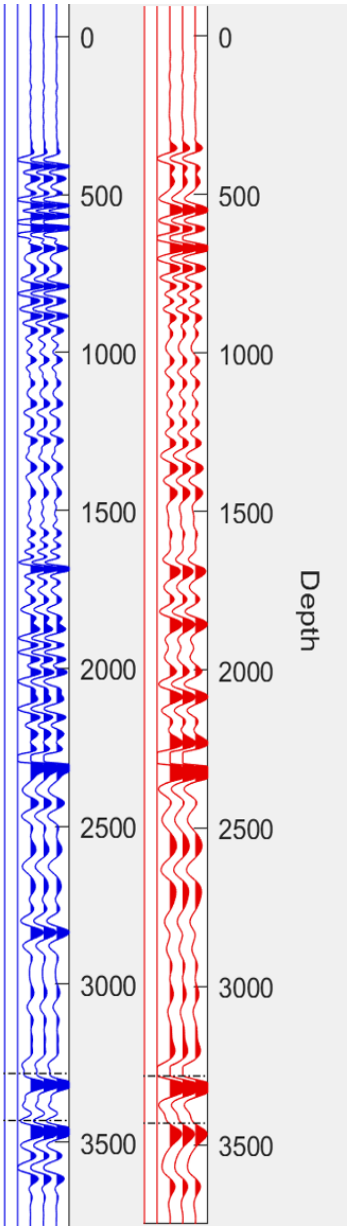

FIG. 8. Polarity flips around the depth of 3750 m in P-S stack when using offset-depth ratio 1.3 and 1.5 for P-P and P-S, respectively

PS DESIGN ANALYSIS

PS Design software allows to run the conventional CMP binning for P-P data and two types of P-S survey design; asymptotic and depth specific. In this part, we will compare and evaluate the fold and azimuth for P-P, P-S asymptotic and depth specific, with and without the optimum bin size.

P-P design

The source and receiver geometry in Figure 3 (bottom) is designed to approximate the same acquisition parameters of the real data, as shown in Figure 9. After designing the geometry, calculating the bin size from the acquisition parameters (30 x 30 m) and estimating the maximum

useable offset from the synthetic seismograms (3000 m), we evaluate the fold, offset range, offset distribution and azimuth distribution maps, shown in Figure 10.

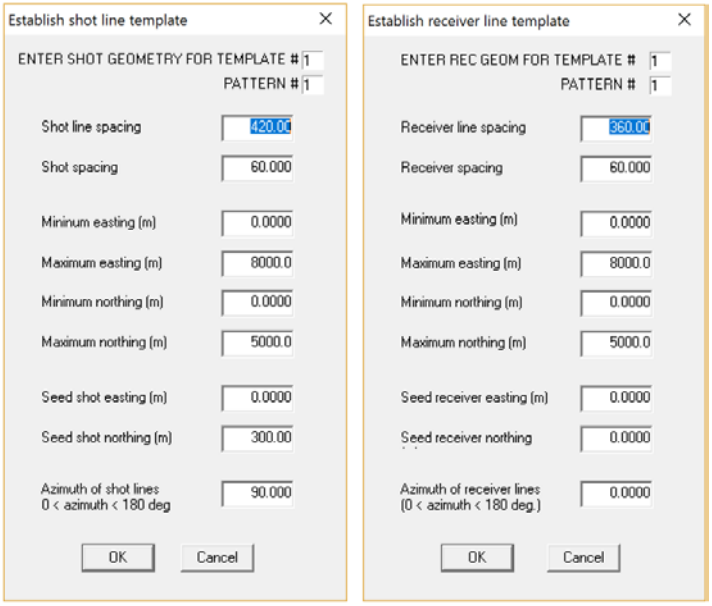

FIG. 9. Shot (left) and receiver (receiver) parameters used to design the geometry

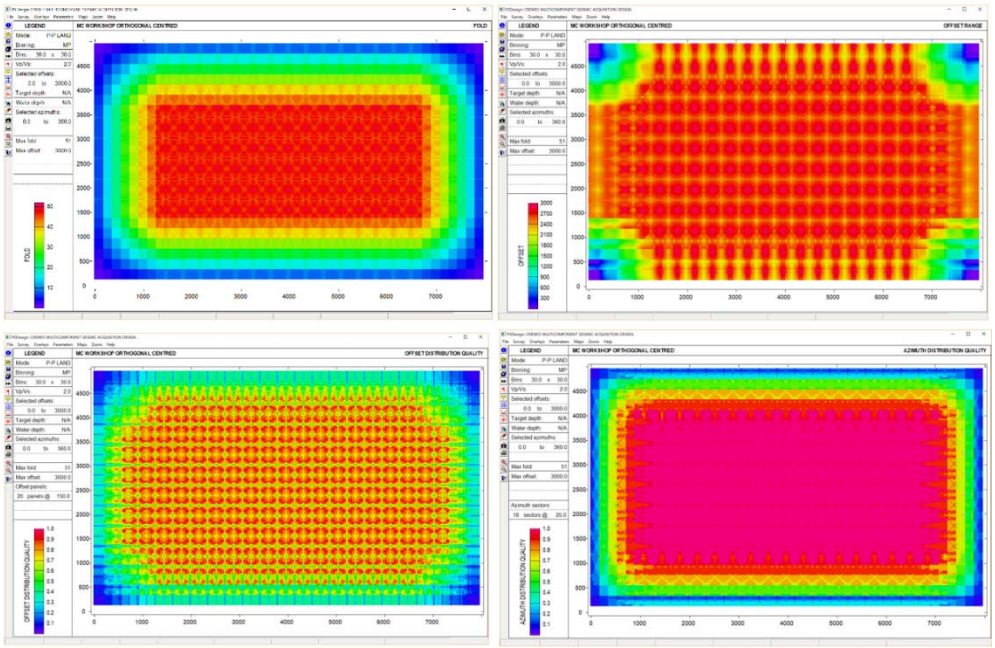

FIG. 10. P-P maps: fold (top left), offset range (top right), offset distribution (bottom left) and azimuth distribution (bottom right)

The maps in Figure 10, shows a good distribution of attributes for the high-fold parts of the whole survey. That is expected as the survey is orthogonal and the grid is binned based on CMP conventional gridding. Further analysis is done by zooming to the middle of the

survey, as in Figure 11, and evaluating the azimuth vs fold and offset vs fold for a single bin as an example.

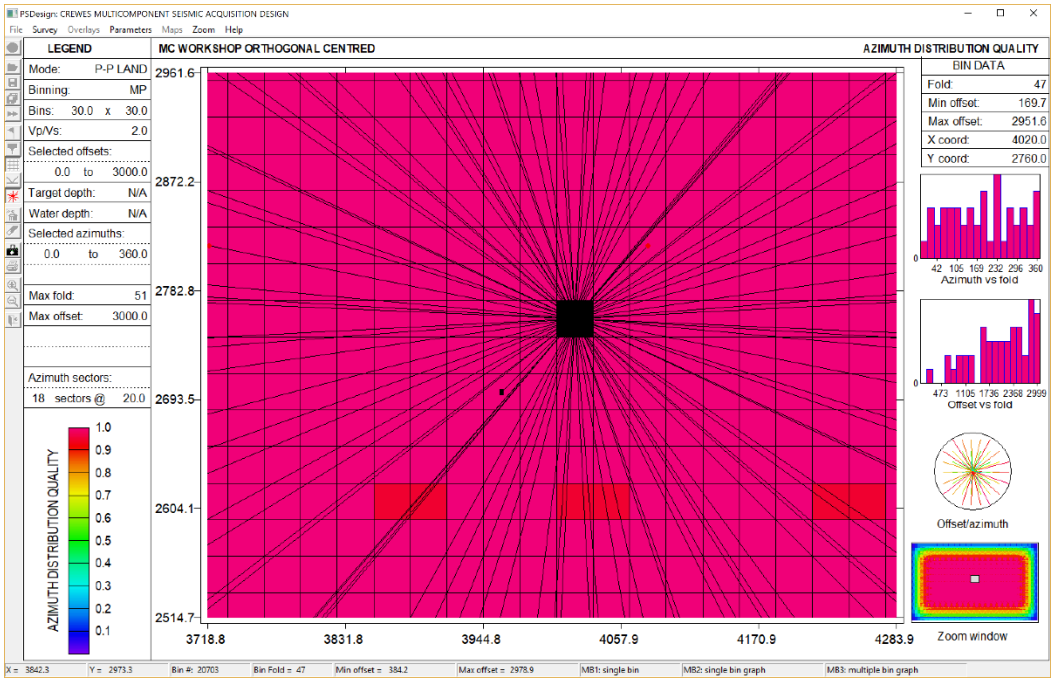

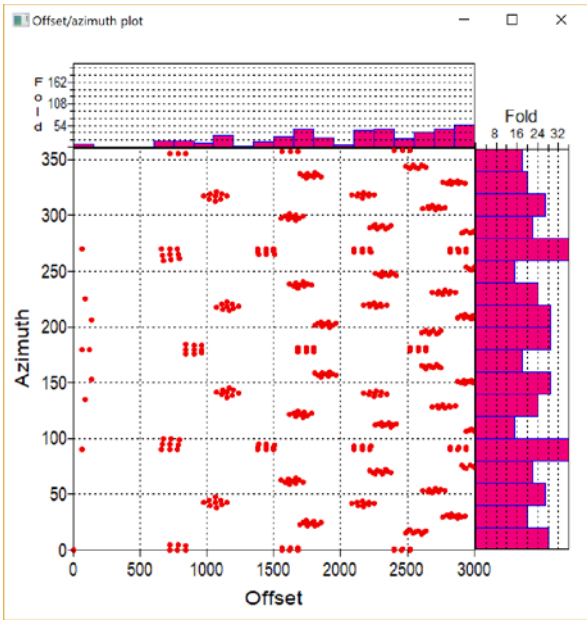

FIG. 11. Azimuth vs fold is almost consistent for a single bin in the middle of the survey (top). More traces from far offsets are contributing to a bin in the middle of the survey (top). A uniform distribution between azimuth and offset (bottom)

P-S design (Asymptotic)

P-S Design offers two types to design the survey for P-S data. The first one is the P-S asymptotic and the second one is P-S depth specific. In this part, we will do the same steps as in P-P design but for P-S asymptotic survey. Same binning and offset parameters in the previous part are used.

In addition, V_p/V_s = 2.0 is provided to the software to calculate the conversion point (V_p/V_s at the depth of interest is 2.01, but P-S Design accepts only one significant figure). It calculates the conversion point according to the equation:

$$Xp = \frac{X}{1 + Vs/Vp}$$

where Xp is the offset from the source to the conversion point, X is the total source-to-receiver offset, and V_s/V_p is the shear-to-compressional wave velocity ratio in the area. This method is not depth variant. Therefore, it requires only a simple calculation for each shot-receiver for the conversion point to be placed in the asymptotic location in the subsurface.

Observing the attributes for this P-S design as we did in the previous one, we notice an increase in the fold shown in Figure 12 (top left). However, irregularities are clearly shown in the middle of the survey (the area of nominal fold) and they are consistent in all attributes.

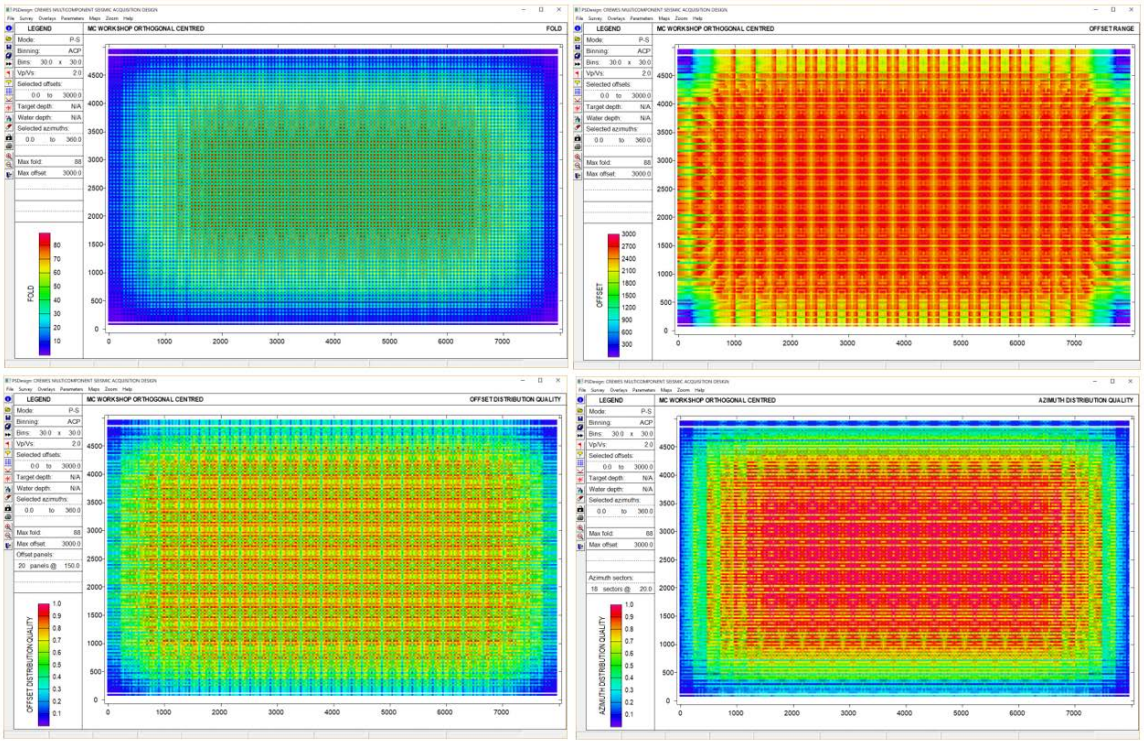

FIG. 12. P-S asymptotic maps: fold (top left), offset range (top right), offset distribution (bottom left) and azimuth distribution (bottom right)

The irregularities in the fold could be better observed in the illumination plot in Figure 13, which is the fold interpolation. Illumination plot is fold mapped to neighboring bins in the case when reflection points are not bin-centered. For other attributes, we evaluated the azimuth vs fold and offset vs fold plots in Figure 14.

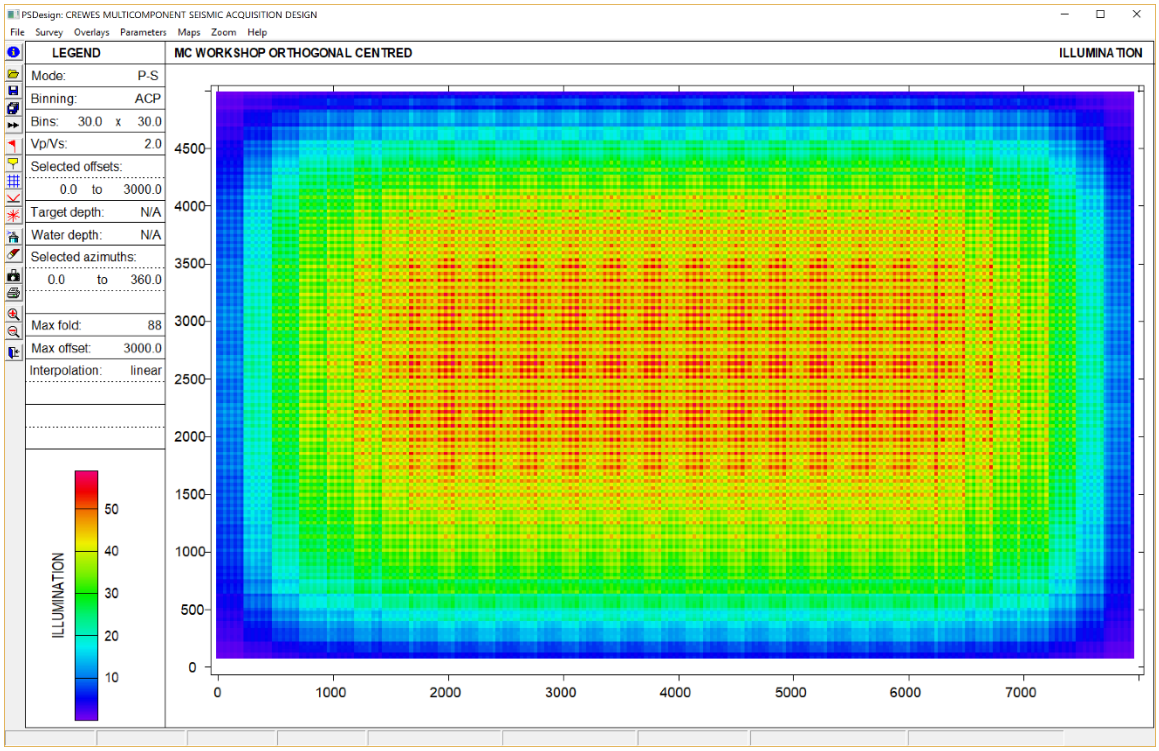

FIG. 13. P-S asymptotic survey illumination map. Irregularities in the fold is clearly shown in the middle of the survey

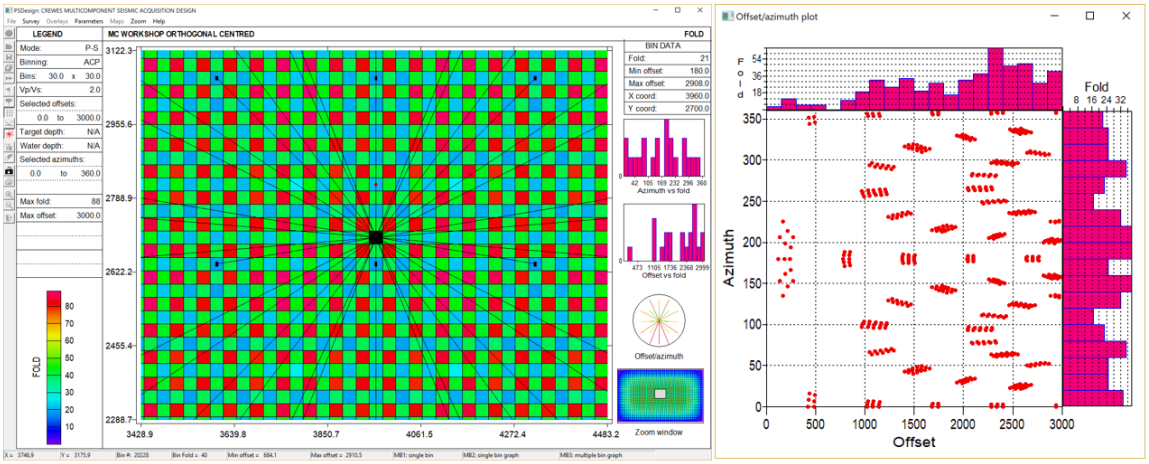

FIG. 14. From the zoomed in fold map (left), fold varies between neighboring bins. Also, a lot of bins have many traces coming from far offsets only (left). A less uniform distribution between azimuth and offset compared to the P-P survey design (right)

One way to fix the issue of irregularities in P-S surveys, is to change the shooting from orthogonal to slanted shot lines. However, that is not an option in this case as the real survey is already conducted as orthogonal. But, we can re-bin the survey to optimum bin size using the following equation (Lawton, 1993):

$$\Delta Xc = \Delta r/(1 + \frac{Vs}{Vp})$$

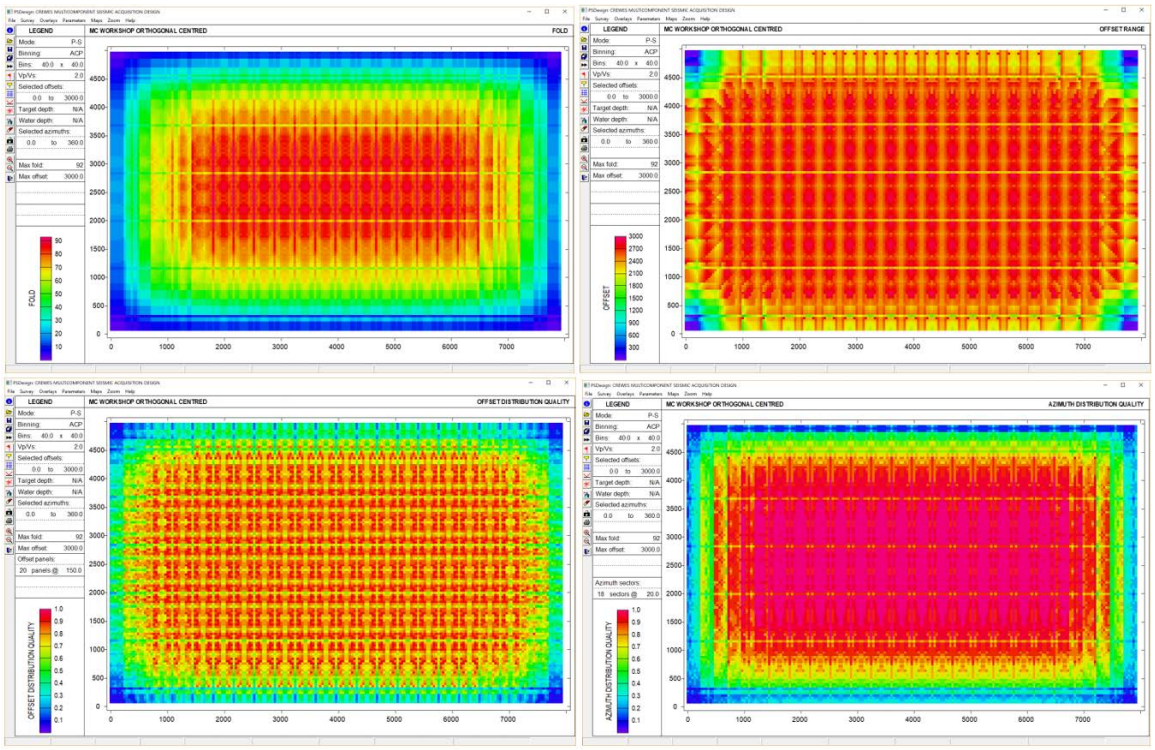

FIG. 15. P-S asymptotic maps after re-binning: fold (top left), offset range (top right), offset distribution (bottom left) and azimuth distribution (bottom right)

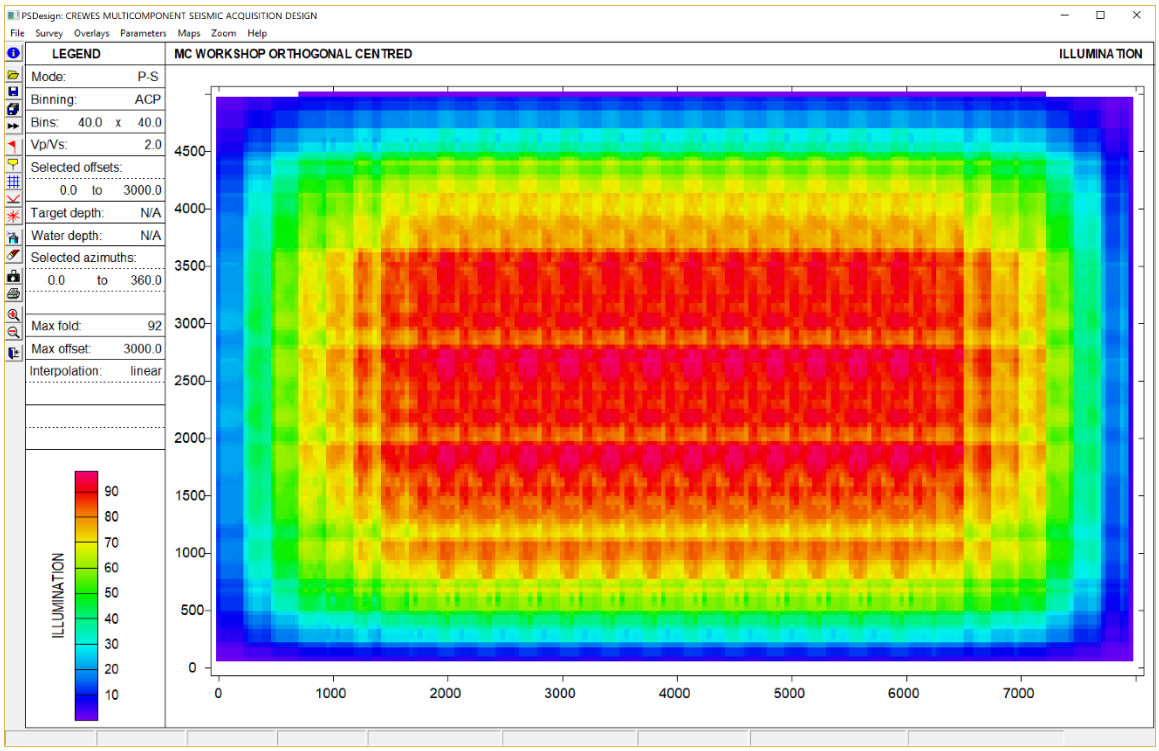

FIG. 16. P-S asymptotic survey illumination map after re-binning. Irregularities in the fold have decreased in the middle of the survey

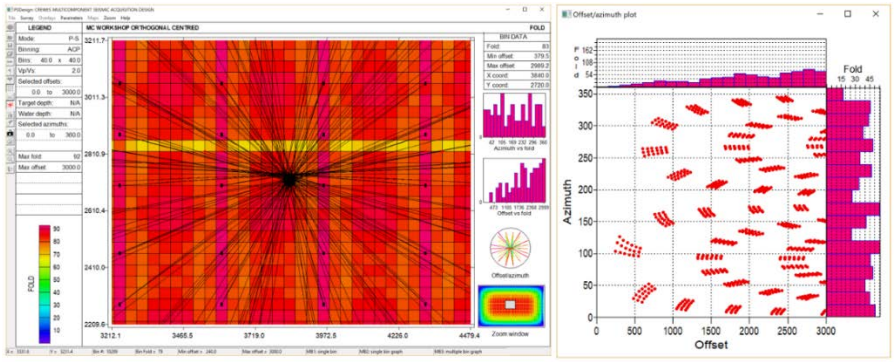

FIG. 17. From the zoomed in fold map (left), fold looks more consistent between neighboring bins than it was before the re-binning. Also, more traces from far offsets are contributing to a bin in the middle of the survey, which helps with fold regularity (left). More uniform distribution between azimuth and offset compared to the P-S survey design before re-binning (bottom)

P-S design (depth-specific)

In this method, we give extra information to the program which is the depth of interest. A drop in the fold is expected as traces from smaller offsets will not be included in the fold. However, this method requires us to know the vertical resolution in our depth of interest by evaluating the fold map at that depth besides other attributes. The depth of interest is between the Devonian Woodbend (3282.7 m) and Duvernay formations (3431.6 m). We selected 3350 m for this evaluation as a depth of interest.

First, we will evaluate the attributes with the conventional CMP bin size (30x30 m). Then, we will re-bin the grid and compare the two. The maps in Figures 18 and 19 show the attributes of this method before re-binning.

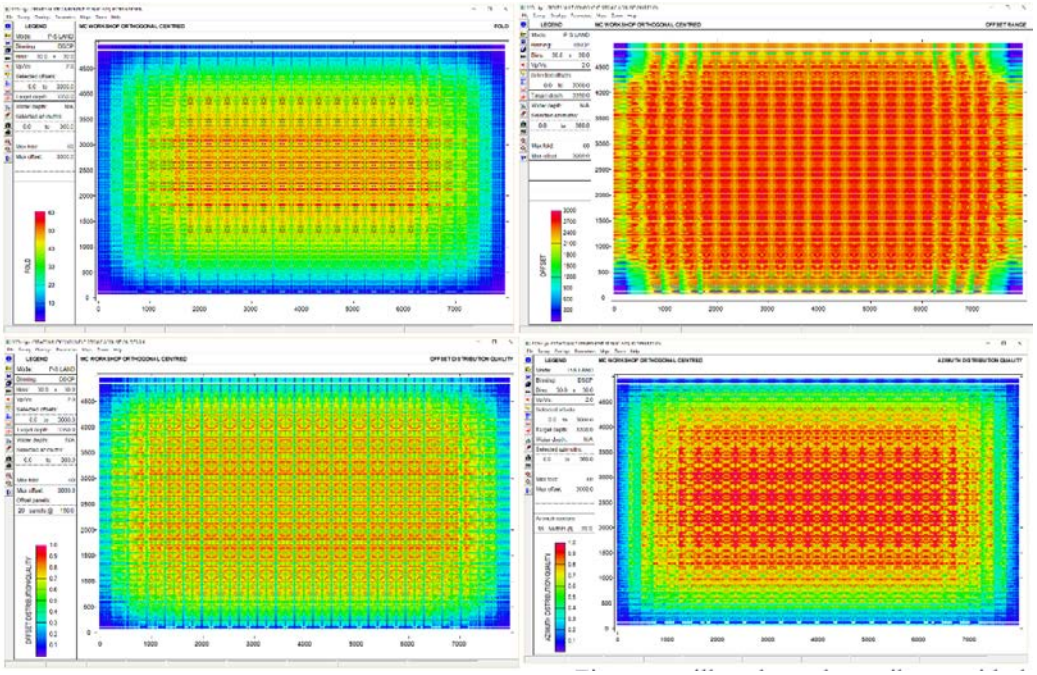

FIG. 18. P-S depth-specific maps: fold (top left), offset range (top right), offset distribution (bottom left) and azimuth distribution (bottom right)

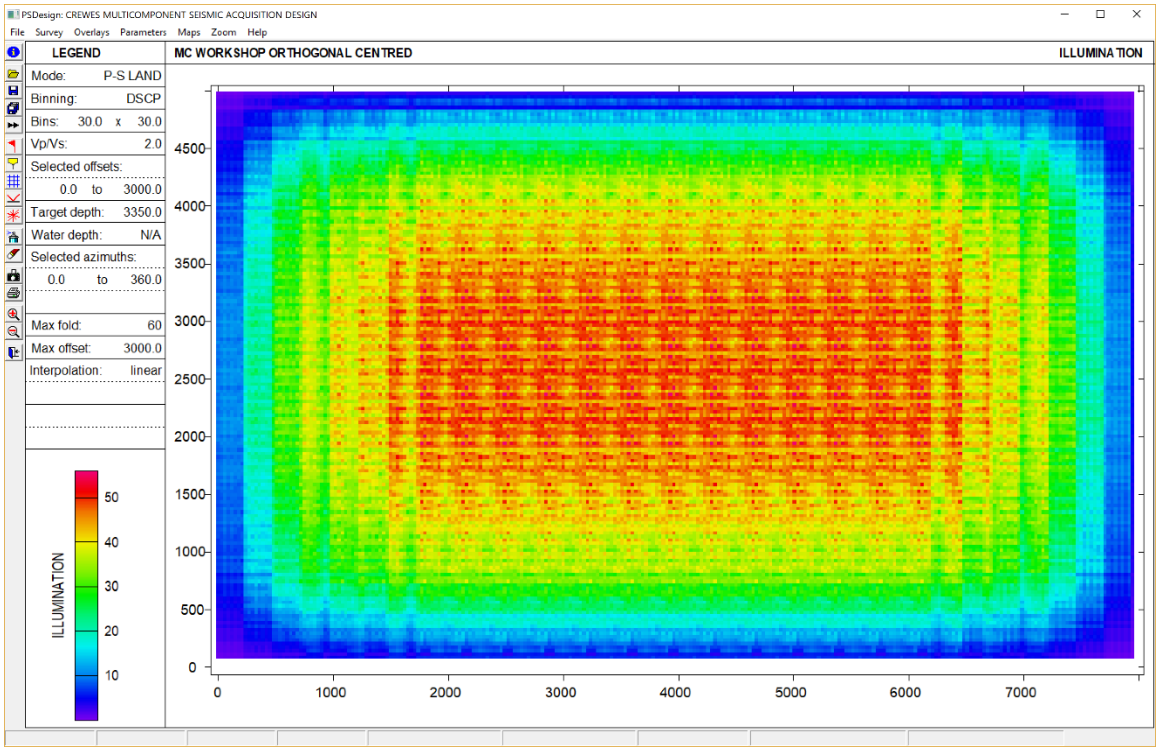

FIG. 19. P-S depth-specific survey illumination map. Irregularities are reduced compared with the asymptotic illumination before the re-binning

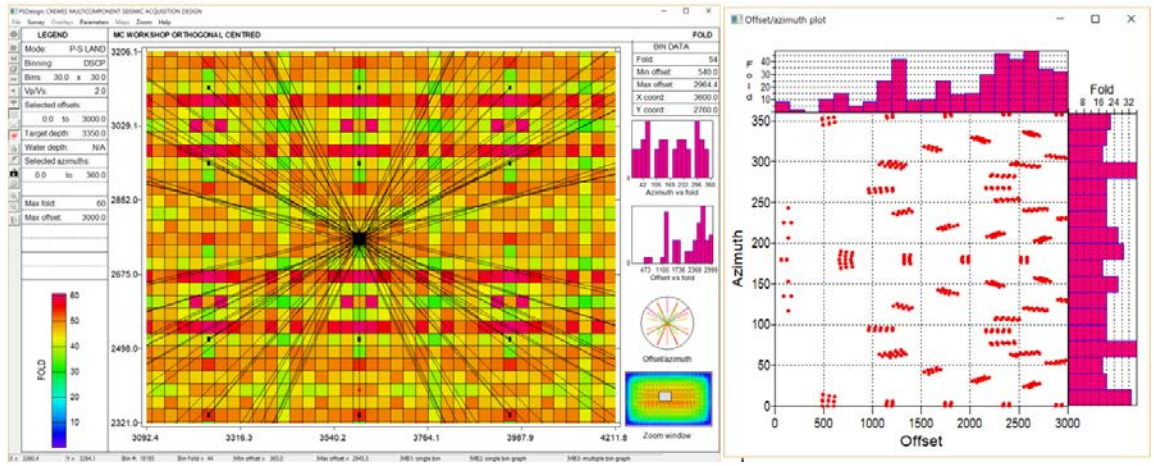

FIG. 20. From the zoomed in fold map (left), fold varies between neighboring bins. The variation is not as big as the asymptotic survey before re-binning. A less uniform distribution between azimuth and offset compared to the P-P survey design (right)

Similar to the P-S asymptotic survey, grid is re-binned with the optimum bin size (40x40 m). The resulted maps are shown in Figures 21 and 22.

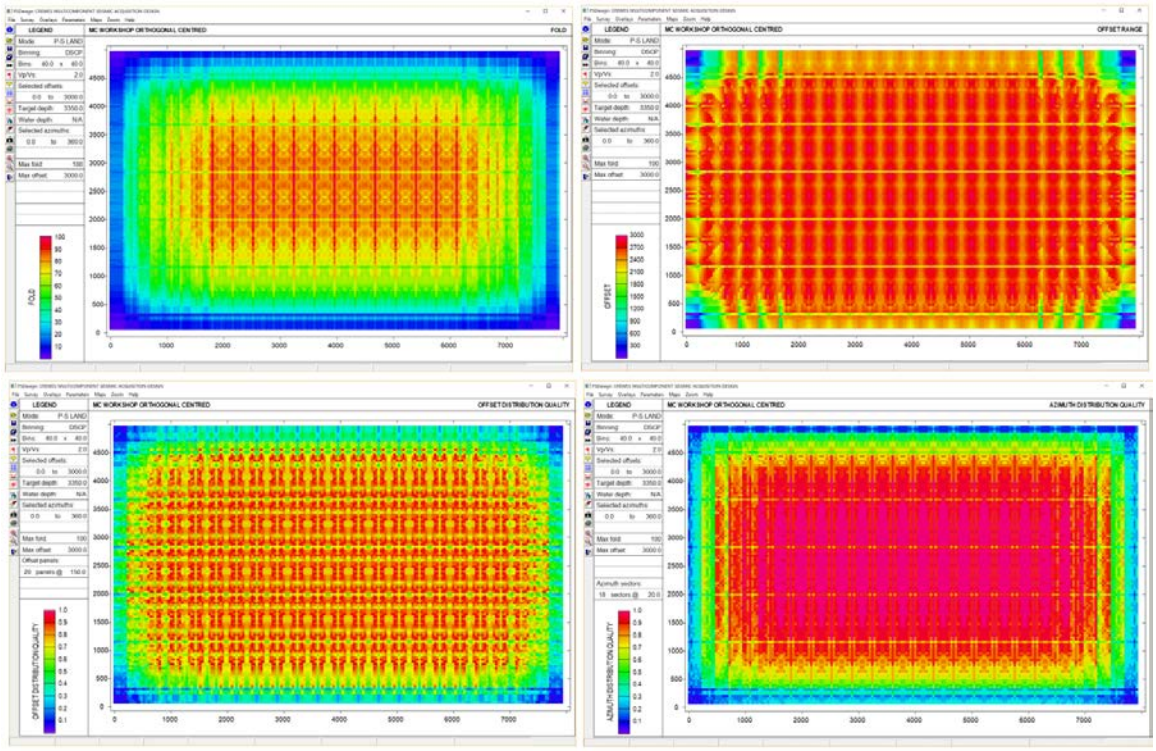

FIG. 21. P-S depth-specific maps after re-binning: fold (top left), offset range (top right), offset distribution (bottom left) and azimuth distribution (bottom right)

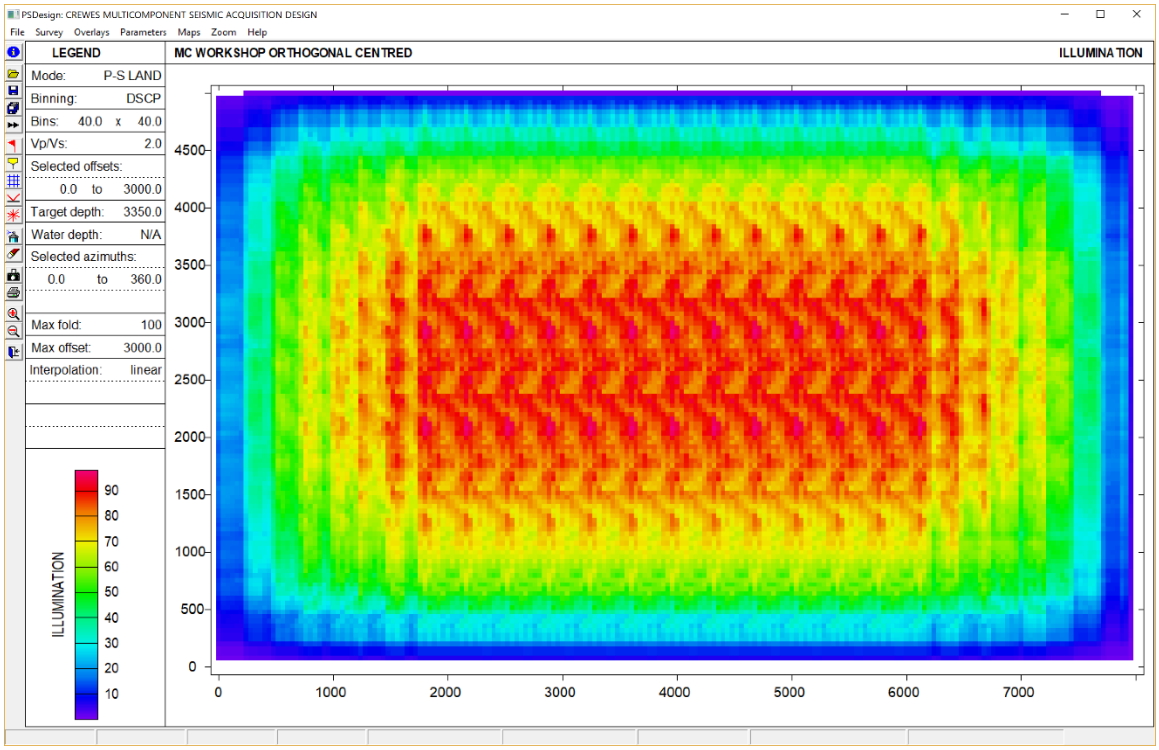

FIG. 22. P-S depth-specific survey illumination map after re-binning. Irregularities in the fold are decreased in the middle of the survey. However, there is a zig zag pattern that was not there before re-binning

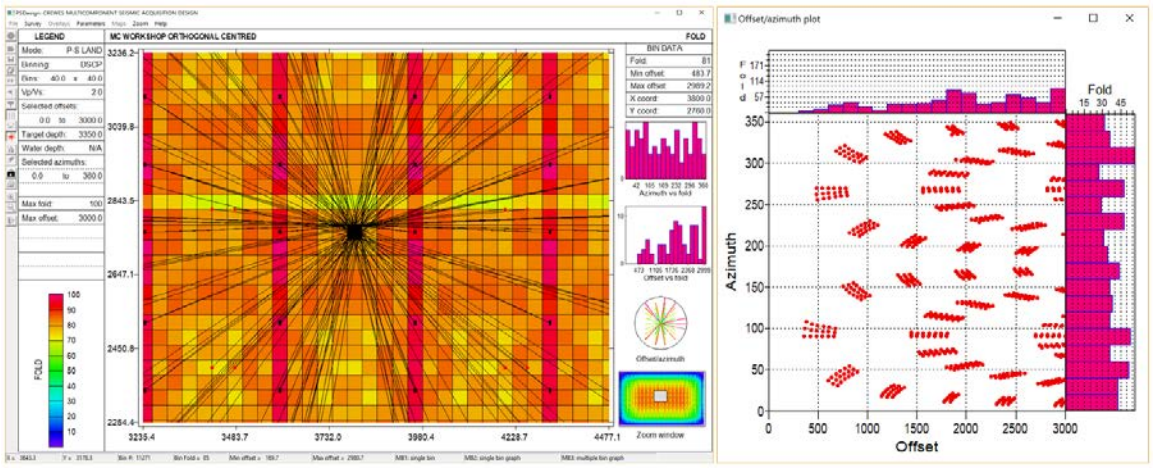

FIG. 23. From the zoomed in fold map (left), fold looks more consistent between neighboring bins than it was before the re-binning. Also, more traces from far offsets are contributing to a bin in the middle of the survey, which helps with fold regularity (left)

CONCLUSION

P-P survey designs are binned using the conventional CMP binning. That is why the fold map and other attribute maps do not have any irregularities. In our case here, the bin size was 30 x30 m and the maximum offset, determined from the synthetic seismograms to be 3000 m. The nominal fold is 51 and it is regular through the nominal fold area in the middle of the survey.

For P-S asymptotic survey, V_p/V_s was provided to calculate the conversion points. The fold increased as expected. However, it was not regular along the nominal fold area. It is due to the change of conversion point locations with depth that the asymptotic method does not account for. One method to solve the issue of irregularities is to re-bin the grid to the optimum bin size. The optimum bin size for this survey parameters is calculated to be 40 x 40 m. After re-binning, fold increased as the larger bins will include more traces. Moreover, the re-binning helped to smooth the irregularities in all attributes consistently, as confirmed in the illumination map.

For P-S depth-specific survey, similar procedures to the P-S asymptotic are followed. Except for this survey, the depth of interest is provided to evaluate the same attributes evaluated before but at specific depth. More regular fold distribution is expected compared to the P-S asymptotic survey is expected. Because all the traces from smaller offsets that do not reach the provided depth are not included in the fold map. However, the fold map shows better regularity than the P-S asymptotic before re-binning. That is because conversion points get closer to each other with depth. After re-binning, same thing happened as in P-S asymptotic survey, fold increased. Furthermore, the illumination map shows better regularity as indicated by the color bar although we see a zig zag pattern in the map.

FUTURE WORK

After evaluating the attributes from different methods, we can do the same on the real data to compare the results. That will help study the effect of the irregular shot-receiver geometry in the real data on the seismic attributes.

Also, attributes could be evaluated using different more sophisticated binning methods like the depth-variant common conversion point. Then, compare the results with both P-S asymptotic and depth-specific results.

ACKNOWLEDGMENT

We would like to thank CREWES sponsors and NSERC through grant CRDPJ 461179-13 for financial support. Further thanks to Ron Weir and Kevin Hall for their guidance and discussions during this research. Lastly, I would like to thank Saudi Aramco for their scholarship support.

REFERENCES

Armin W Schafer, A comparison of converted –wave binning methods using synthetic model of the High wood structure, Alberta Crews Research Report Vol4(1992)

Cordsen, A, Galbraith, M., and Peirce, J., 2000, Planning land 3-D seismic surveys, Geophysical Developments No. 9, Hardage, B.A., ed., Society of Exploration Geophysicists.

Cordsen, A., and Lawton, D.C., 1996, Designing 3-component 3D seismic surveys: 66th Annual Meeting of the Society of Exploration Geophysicists, Expanded Abstracts, 81-83.

Lawton, Don C. "Optimum bin size for converted-wave 3-D asymptotic mapping." CREWES Research Report (University of Calgary) 5.28 (1993): 1-14.

Weir, Ronald M., et al. "Inversion and interpretation of seismic-derived rock properties in the Duvernay play." Interpretation 6.2 (2018): SE1-SE14.

Zuleta, Liliana M., and Don C. Lawton. "PS survey design." SEG Technical Program Expanded Abstracts 2011. Society of Exploration Geophysicists, 2011. 127-131.